Effects of Niobium Additions on Textures and Mechanical Properties of Zirconium Alloys

Sheikh T. MAHMOOD, J. RAVI, K. Linga MURTY
North Carolina State University, Raleigh, NC USA

ABSTRACT

Crystallographic texture and mechanical anisotropy of Nb-modified zirconium alloys were investigated on 3 different alloys. The mechanical anisotropy parameters were determined using mechanical testing of gridded tensile samples. The textures were characterized by x-ray pole figure measurements and crystallite orientation distribution functions [CODFs]. The CODFs were combined with crystal plasticity model to predict the anisotropy parameters based on the dominance individually of basal, prism and pyramidal slip systems.

1 INTRODUCTION

Zr-Nb alloys are now being considered to replace Zircaloy materials in LWR's, and various nuclear reactor manufacturers are considering binary and ternary alloys of Zr and Nb. In addition, some nuclear reactor vendors [such as Westinghouse] very recently announced the introduction of new generation alloys such as Zirlo™ alloys, which are Nb-modified Zircaloys (Sabol et al. 1989). These materials exhibit resistance to in-reactor corrosion and oxidation particularly at long exposures. However, currently adequate information on the effect of Nb on crystallographic textures and accompanying mechanical anisotropy is not available. This information is very important for selecting optimum fabrication parameters (textures) as well as for accurate prediction of the dimensional stability of the final product (cladding, pressure tubes, spacer grids, channels, etc.). The purpose of this study has been to evaluate the effect of Nb on the crystallographic texture, mechanical anisotropy, and formability of zirconium alloys.

2 EXPERIMENTAL ASPECTS

Alloys with different compositions have been procured in the form of thin sheets of thickness varying from 0.75 to 0.85 mm. Table 1 gives the chemical compositions of these alloys.

Table 1. Chemical Composition (wt%) of Zr-Nb Alloys

	Nb	Sn	Fe	Cr	Mo	Ni	Zr
Alloy 1	1.0	1.5	0.15	0.1	-	0.05	Balance
Alloy 2	0.3	1.5	-	-	0.3	-	Balance
Alloy 3	1.0	1.0	0.2	-	-	-	Balance

SMiRT 11 Transactions Vol. C (August 1991) Tokyo, Japan, © 1991

Alloy 1 is Zircaloy-2 with 1.0% Nb while Alloys 2 and 3 are Zr-Nb alloys with different compositions. Alloys 1 and 3 are in cold-worked condition, and Alloy 2 is recrystallized. The textures and anisotropy tests were performed on materials in the as-received conditions. Crystallographic textures were characterized by x-ray methods using both the inverse and direct pole figures and the details of the analyses and methodology were already published (Mahmood and Murty 1989). The random intensities were obtained from inverse pole figure data obtained along the three orthogonal directions, rolling [RD], transverse [TD] and thickness or normal [ND] directions. Basal, prism and pyramidal pole figures were obtained using direct pole figure technique from which the CODFs were evaluated as described earlier. Tensile tests were performed on gridded samples of 31.75 mm gauge length and 6.35 mm wide fabricated with tensile axis along both RD and TD and the samples were electroetched with square grids of 1.27 mm^2. The changes in the grid dimensions along the tensile and transverse directions yielded information on the tensile and contractile strains which made it possible to evaluate the anisotropy parameters, which are the transverse contractile strain ratios, as a function of the tensile strain up to fracture.

3 EXPERIMENTAL RESULTS AND DISCUSSION

3.1 Crystallographic Texture

Direct pole figure technique is used in determining the basal, prismatic and pyramidal pole figures and either one or a combination of samples were used. Fig.1a shows basal, prism, and pyramidal pole figures for Alloy 1, where RD and TD refer to the rolling and transverse directions, respectively, and ND is always at the center. The isointensity contours are plotted in the units of times random. This material exhibits typical features of cold-worked texture in zirconium alloys. The basal pole figure shows bimodal texture with the basal pole maxima at about ±30 degrees from the ND in the ND-TD plane with a maximum intensity of 6.5. The prism poles are aligned along or around the rolling direction with a maximum intensity of about 4.5, while the pyramidal poles are more spread out. The crystallographic texture pole figures for Alloy 2 is typical of recrystallized Zircaloy (Fig.1b) with the prism pole peaks displaced from the RD. Fig.1c compiles basal, prism, and pyramidal pole figures, respectively, for Alloy 3, which is in the cold-worked condition and contains 1.0% Nb and Sn along with 0.2% Fe. The basal pole figure for this alloy exhibits significant differences when compared with the typical bimodal texture of Zircaloys. The intensity maxima are at about 15 degrees from the ND in the ND-RD plane, and at about 27 degrees from the ND in the ND-TD plane, with a maximum intensity of 4.5. The prism and pyramidal pole figures for this alloy exhibit the typical features of cold-worked texture.

A crystallite orientation distribution function (CODF) is defined as a distribution function which gives the probability that a crystallite lies within a certain range of orientations (θ,ψ,ϕ) with respect to the specified coordinates, which are generally the processing axes of the material (ND, RD, and TD for a sheet) and is given as a series of generalized spherical harmonics (Murty 1989),

$$\omega(\theta, \psi, \phi) = \sum_{l=0}^{\infty} \sum_{m=-l}^{l} \sum_{n=-l}^{l} W_{lmn} Z_{lmn} (\cos\theta) e^{-im\psi} e^{-in\phi}, \qquad (1)$$

where W_{lmn} are the appropriate series coefficients and Z_{lmn} are the augmented Jacobi polynomials. In the present study, three pole figures (basal, prismatic and pyramidal) were used to evaluate the series coefficients W_{lmn} up to $l=16$. The error caused by truncating l at 16 is generally insignificant compared to the errors inherent in experimental texture measurements.

Physical and mechanical properties of single crystals are anisotropic and this extends to the bulk properties of the polycrystals whenever preferred orientations are present. To the first order, the bulk property is related to the microscopic property, $\rho(\theta,\psi,\phi)$, by statistical averaging using the CODF so that the average property of the polycrystalline aggregate, $\langle\rho(\theta,\psi,\phi)\rangle$, is given by

$$\langle\rho(\theta,\psi,\phi)\rangle = \int_0^{2\pi}\int_0^{2\pi}\int_{-1}^{1} \rho(\theta,\psi,\phi)\ \omega(\theta,\psi,\phi)\ d(\cos\theta)\, d\psi\, d\phi \qquad (2)$$

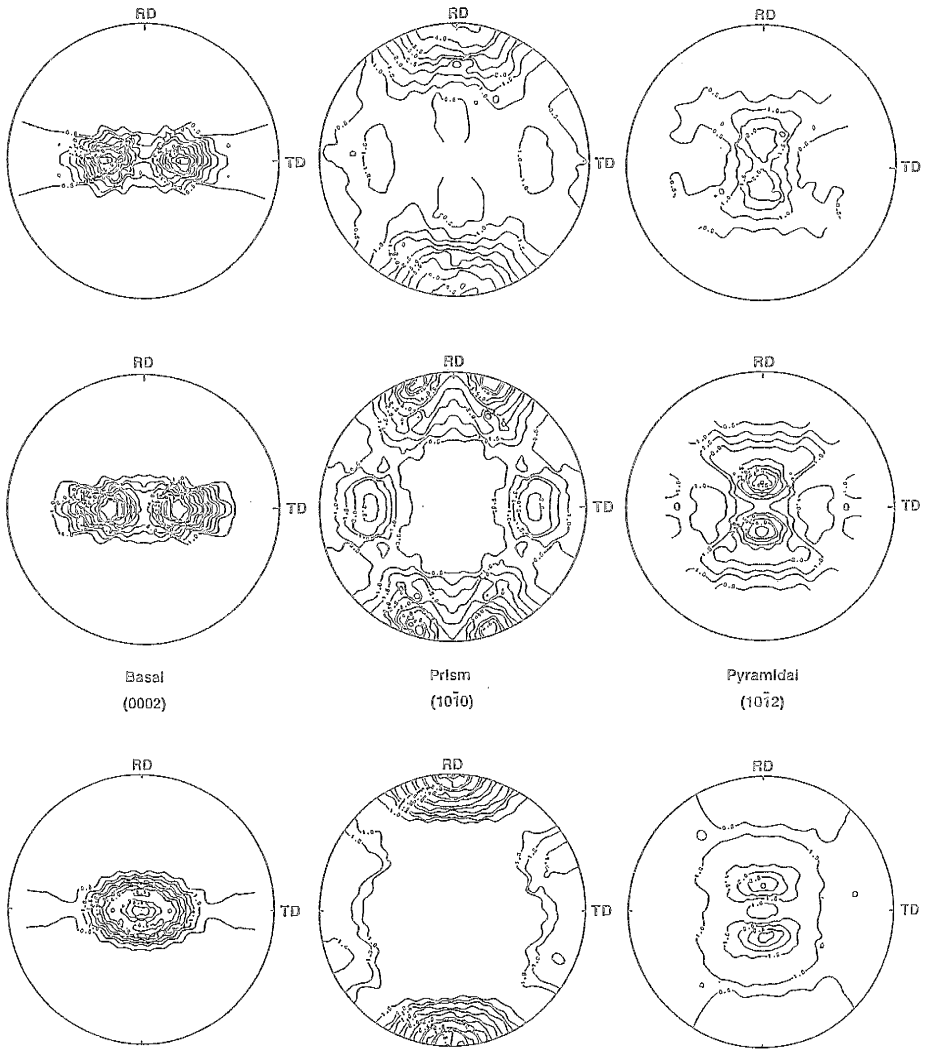

Fig.1. Pole Figures for Alloys 1 (a, top), 2 (b, middle) and 3 (c, bottom)

3.2 CODF-Plasticity Model

Following the modified von-Mises - Hill yield criterion, a generalized stress, σ_g, is defined as the uniaxial stress along the axial direction so that the yield criterion reads as follows:

$$\sigma_g^2 = \frac{R(\sigma_{ND} - \sigma_{TD})^2 + RP(\sigma_{TD} - \sigma_{RD})^2 + P(\sigma_{RD} - \sigma_{ND})^2}{P(R+1)} \qquad (3)$$

where σ_{ND}, σ_{TD} and σ_{RD} are the stresses along the normal, transverse and rolling directions of the sheet, and R and P are the coefficients of anisotropy.

Once the orientation distribution of crystallites in the polycrystalline materials is evaluated and the appropriate CODF is known, the crystallite behavior in each orientation can be weighted by the volume fraction of crystallites in that orientation so that the behavior of the polycrystalline aggregate can be predicted. If m is the strain-rate sensitivity, the shear strain-rate on the sth slip system can be expressed as,

$$\tau^s = A\,\tau_o^s \left[\dot{\gamma}^s\right]^m \qquad (4)$$

where τ_o^s is the reference shear stress on the sth slip system, m the strain-rate sensitivity and A the reference strain-rate. In the upper-bound method, the strain state in each crystallite is regarded identical to the applied macroscopic strain tensor and the stress state is calculated using the constitutive equation. The bulk stress state is then obtained by averaging the stress state of the individual grains weighted by CODF using Eq. 2. Three different slip modes are considered in the present analyses: basal ({00.1}<11.0>), prism ({10.0}<11.0>) and pyramidal ({11.2}<11.3>). Values of the reference stresses (τ_o) are chosen to emphasize the contribution of individual or particular combinations of slip modes to the polycrystalline behavior.

3.3 Mechanical Properties

Fig.2 depicts a typical sequence of grid photographs taken during a tensile test and the grid size measurements yield the true transverse and contractile strains. This technique can be used to study the spatial and temporal strain distributions. Table 2 summarizes the mechanical properties data and the yield strengths along the transverse directions of the sheet for all the alloys are seen to be higher than those along the rolling direction. Whereas, the tensile strengths [UTS] along the rolling direction of the alloys 1 and 2 are higher than those along the transverse direction, illustrating that the material exhibits anisotropy in the mechanical strength as well as in the rates of work-hardening. The tensile strengths of the alloy 3, however, are essentially identical indicating planar isotropy and the rates of strain hardening are also similar along RD and TD.

3.4. Anisotropy Parameters

The grid analysis technique enables an evaluation of the mechanical anisotropy parameters R and P and the formability parameter E. The anisotropy parameters, R and P, are also given by the contractile strain ratios for tests along RD and TD respectively (Mahmood and Murty, 1989). These parameters were determined by measuring the axial tensile and transverse contractile strains in the grid elements which ultimately fractured in the RD and TD specimens. Figures 3a and 3b show the width contraction as a function of longitudinal elongation for both the RD and TD specimens for Alloy 3; similar data were obtained on the other two alloys also. A linear variation is noted between the contractile and tensile strains and the slopes of these lines were used to determine the R and P parameters from which the formability parameter, E, is calculated,

$$B = \frac{\sigma_I}{2\sigma_{IV}} = \sqrt{\left\{\frac{(R+1)(R+4RP+P)}{4R(R+P+1)}\right\}} \quad . \qquad (5)$$

Here σ_I and σ_{IV} are the plane strain stress in the first quadrant and the equibiaxial stress in the 4th quadrant respectively. The significance of the parameter B lies in the fact that higher the B value the better the cup formability of the material. Table 3 summarizes the experimental data on these parameters.

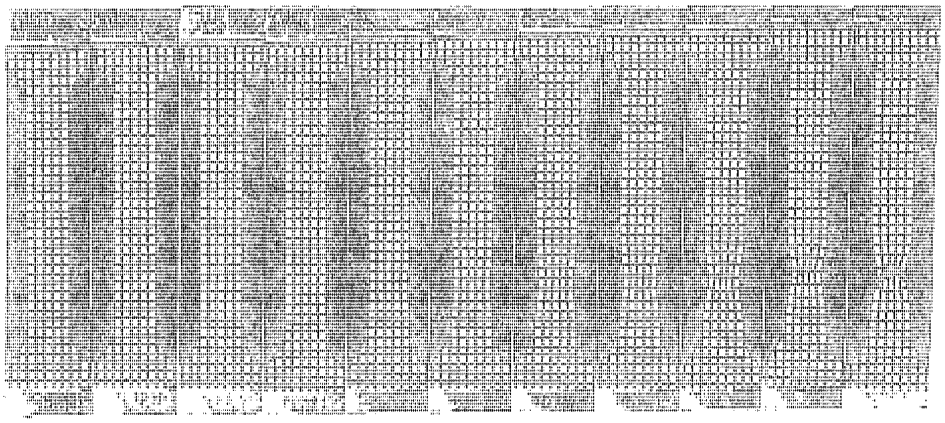

Strain (%) 0 3.1 4.4 5.7 6.9 7.9 9.2 10.1 11.0 11.9 12.1

Fig.2. A typical sequence of grid photographs taken during a tensile test

Table 2. Mechanical Properties

Property	Alloy 1		Alloy 2		Alloy 3	
	RD	TD	RD	TD	RD	TD
0.2% yield strength (MPa)	489±17	650±23	565±20	676±24	892±31	907±32
Tensile Strength (MPa)	736±26	672±23	712±25	660±23	1116±39	1088±38
Total Elongation (%)	.24±.02	.29±.03	.30±.02	.22±.03	.12±.01	.11±.01
Strain Hardening Exponent (n)*	.21±.02	.08±.01	.17±.02	.05±.02	.06±.01	.05±.01
Strength Coefficient (K, MPa)*	1346±47	885±31	1154±47	749±26	1406±49	1308±46

* $\sigma = K\,\varepsilon^n$

The plasticity model was used in conjunction with the derived CODFs for the alloys to predict these parameters based on the dominance of prism, basal and pyramidal slip by appropriately adjusting the reference stress in Eq.4 and for the strain-rate sensitivity, m, of 0.01 appropriate for ambient deformation of Zirconium alloys. The predicted values are also included in the Table 3 and the experimental results agree with the model predictions based on the dominance of prism slip. For the Alloy 1, however, which is in the cold-worked condition, the correlation is poor although the experimental results are still closer to the predictions based on the prism slip dominance. The present poor correlation noted for the cold-worked sheet might have resulted from the additional contribution from basal slip to that dominated by the prism system.

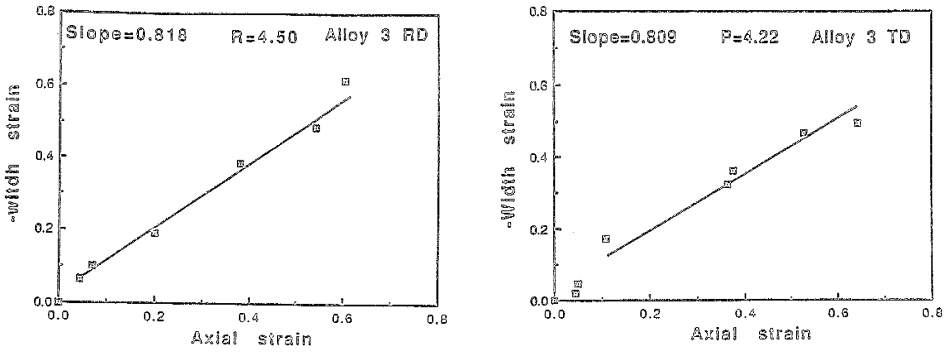

Fig.3. Contractile width strain versus longitudinal tensile strain along RD and TD

Table 3. Anisotropy and Formability Parameters

Material	Slip System	R	P	B
Alloy 1	Prism	2.32	6.36	1.58
	Basal	0.74	0.14	0.64
	Pyramidal	0.48	0.47	0.86
	Experimental	1.50±0.08	4.27±0.21	1.93±0.09
Alloy 2	Prism	2.11	4.64	1.48
	Basal	1.58	0.31	0.74
	Pyramidal	0.55	1.06	1.03
	Experimental	2.33±0.12	4.27±0.18	1.93±0.10
Alloy 3	Prism	4.84	4.56	1.68
	Basal	2.15	0.38	0.78
	Pyramidal	0.24	0.23	0.78
	Experimental	4.50±0.23	4.22±0.21	1.63±0.12

4 ACKNOWLEDGMENTS

Financial supports through grants from the National Science Foundation and the Electric Power Research Center at NCSU are gratefully acknowledged.

5 REFERENCES

Mahmood, S.T. and Murty, K.L. (1989). Localized Plastic Flow, Anisotropic Mechanical Properties and Crystallographic Texture in Zircaloy Sheet. J. Mat. Eng., Vol.11, pp.315-329.

Murty, K.L. (1989). Applications of Crystallographic Textures of Zirconium Alloys in the Nuclear Industry, in *Zirconium in the Nuclear Industry: Eighth International Symposium,* ASTM STP 1023, American Society for Testing and Materials, Philadelphia, pp. 570-595.

Sabol, G.P., Kilp, G.R., Balfour, M.G. and Roberts, E. (1989). Development of a Cladding Alloy for High Burnup, in *Zirconium in the Nuclear Industry: Eighth International Symposium,* ASTM STP 1023, ASTM, Philadelphia, pp. 227-244.